



TITLE:

Visualization of solute diffusion into cell walls in solution-impregnated wood under varying relative humidity using time-of-flight secondary ion mass spectrometry

AUTHOR(S):

Zheng, Peiming; Aoki, Dan; Seki, Masako; Miki, Tsunehisa; Tanaka, Soichi; Kanayama, Kozo; Matsushita, Yasuyuki; Fukushima, Kazuhiko

CITATION:

Zheng, Peiming ...[et al]. Visualization of solute diffusion into cell walls in solution-impregnated wood under varying relative humidity using time-of-flight secondary ion mass spectrometry. Scientific Reports 2018, 8: 9819.

ISSUE DATE:

2018-06-29

URL:

<http://hdl.handle.net/2433/232638>

RIGHT:

This article is licensed under a Creative Commons Attribution 4.0 International License, which permits use, sharing, adaptation, distribution and reproduction in any medium or format, as long as you give appropriate credit to the original author(s) and the source, provide a link to the Creative Commons license, and indicate if changes were made. The images or other third party material in this article are included in the article's Creative Commons license, unless indicated otherwise in a credit line to the material. If material is not included in the article's Creative Commons license and your intended use is not permitted by statutory regulation or exceeds the permitted use, you will need to obtain permission directly from the copyright holder. To view a copy of this license, visit <http://creativecommons.org/licenses/by/4.0/>; © The Author(s) 2018.

SCIENTIFIC REPORTS

OPEN

Visualization of solute diffusion into cell walls in solution-impregnated wood under varying relative humidity using time-of-flight secondary ion mass spectrometry

Peiming Zheng¹, Dan Aoki², Masako Seki¹, Tsunehisa Miki¹, Soichi Tanaka³, Kozo Kanayama³, Yasuyuki Matsushita² & Kazuhiko Fukushima²

The purpose of the present study is to clarify the diffusion of non-volatile substances into cell walls during the conditioning procedure under varying relative humidities (RH). In this paper, wood blocks were impregnated using an aqueous solution of melamine formaldehyde (MF), and they were subsequently conditioned under RHs of 11, 43, and 75%. The solute that diffused into the cell walls was visualized using time-of-flight secondary ion mass spectrometry (TOF-SIMS). The volumetric relative swelling of the samples during the conditioning procedure was calculated. The results showed increased cell wall swelling at higher RH, which may have been caused by higher MF diffusion into the cell walls and/or higher moisture content. Cryo-TOF-SIMS measurements showed that more cell cavities were unfilled with MF at higher RH, indicating that most of the MF diffused from the cell cavities into the cell walls. The relative intensity of MF in the cell walls of the cured samples was evaluated from dry-TOF-SIMS images, which showed a higher relative intensity of MF in the cell walls at higher RH. With the ability to visualize and semi-quantitatively evaluate the solute in cell walls, TOF-SIMS will serve as a powerful tool for future studies of solute diffusion mechanisms in solution-impregnated wood.

Treatment using non-volatile substances is an effective method for reducing the undesirable properties of wood materials, such as “non-homogeneity, dimensional instability in moist environments, and susceptibility to sun-light, fungi, and insects”^{1,2}. Wood properties (e.g., mechanical properties and dimensional stability) have been significantly improved by treatment with appropriate substances in previous studies^{3–6}. It has been shown that depositing solute within wood cell walls rather than in cell cavities results in a high decay resistance of the wood as well as an improvement in its mechanical strength and dimensional stability^{6–9}. Thus, maximizing the solute amount in cell walls is important for ensuring treatment efficiency^{2,6}.

Treatment of wood with non-volatile substances includes impregnation and conditioning^{2,6}. The mechanism of solute diffusion into the cell wall has been suggested by Stamm¹⁰ and Tanaka *et al.*^{2,6}: “(i) During impregnation, the solution permeates the cell walls and cell cavities uniformly. (ii) During conditioning, a greater amount of solvent evaporates from the cell cavities compared with that from the cell walls, which results in higher concentration of solute in the cavities compared with that in the walls. This concentration difference causes the diffusion of the solute from the cavities to the walls.” It was concluded that the amount of solute diffused into the cell wall is determined by two factors, the difference in solute concentration between the cell cavities and walls and solute diffusivity into the cell walls. Tanaka *et al.*² concluded that both factors are affected by “solution conditions (such as the concentration and type of solute and solvent), material conditions (such as wood species and dimension), and atmospheric conditions (such as temperature and vapor pressure of the solvent)”. Optimizing the atmospheric conditions is more feasible, because the other conditions often depend on the required properties of the

¹Structural Materials Research Institute, National Institute of Advanced Industrial Science and Technology, Nagoya, 463-8560, Japan. ²Graduate School of Bioagricultural Sciences, Nagoya University, Nagoya, 464-8601, Japan.

³Research Institute for Sustainable Humanosphere, Kyoto University, Uji, 611-0011, Japan. Correspondence and requests for materials should be addressed to P.Z. (email: zhengpm@hotmail.com)

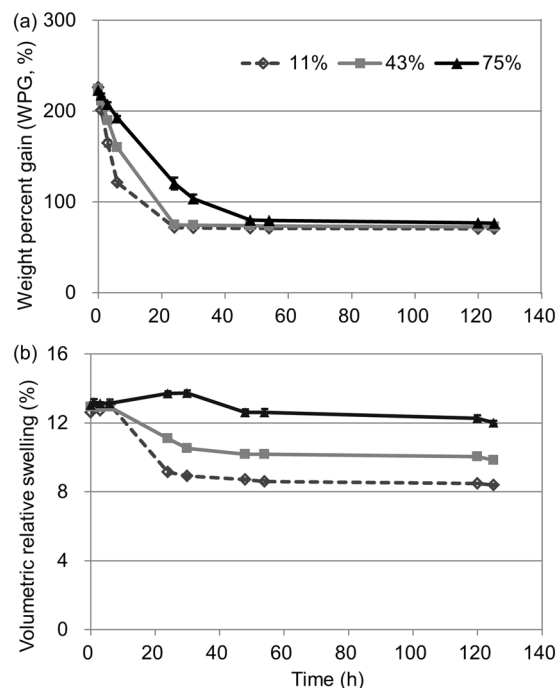


Figure 1. Temporal variability of (a) weight percent gain and (b) volumetric relative swelling of the MF-impregnated samples conditioned at various RHs (11, 43, and 75%). The bars show the standard deviation from three replicates.

treated materials^{2,11}. Therefore, there exists the possibility of maximizing the solute amount in cell walls by optimizing the vapor pressure of the solvent [i.e., the relative humidity (RH) of the aqueous solution].

To investigate the diffusion of solute into the cell wall, it is necessary to choose an appropriate method, which measures its amount and distribution in the cell walls. Tanaka *et al.*⁶ estimated the solute in cell wall by the dimensions of the solution-impregnated wood with polyethylene glycol (PEG). Images from micro-focus X-ray computed tomography (CT) were also used to investigate the resin polymer distribution in cell cavities². However, the resin distribution in the cell walls could not be evaluated. Furuno *et al.*³ investigated the penetration of solute into wood cell walls using electron probe X-ray microanalysis (EPMA) and a m-Bromophenol-formaldehyde resin was used to detect the presence of resin by bromine signals. However, the drying procedure was conducted on samples in these studies. Although the amount of solute diffusing into the cell walls was considered to be small during the drying procedure^{2,12}, drying and curing procedures lead to shrinkage of samples and/or condensation of the solute [e.g., while forming methylene linkages during curing of melamine formaldehyde (MF)]¹³. Thus, solute diffusion into the cell wall affected by RH during the conditioning procedure could not be directly measured.

In the present study, time-of-flight secondary ion mass spectrometry (TOF-SIMS) was employed to map the solute distribution in the cell walls of impregnated wood. TOF-SIMS is an analytical technique having high mass and spatial resolution, and provides semi-quantitative information on the chemical features of the surface of untreated solid samples^{14–19}. TOF-SIMS has been successfully used to visualize the solute distribution in solution-impregnated wood^{20,21}. The sample preparation process is quite important to visualize the actual distribution of the target chemicals²². To avoid movement, draining, or change of the water-soluble chemicals during additional drying process, cryo-TOF-SIMS with frozen samples was recently developed^{15,23,24}.

In the present study, MF was used as the solute in the impregnation treatment. It was reported that, “as one of the hardest and stiffest isotropic thermosetting polymeric materials, MF provides various material advantages for improving wood properties, such as transparency, thermal stability, scratch resistance, moisture resistance, and surface smoothness”^{13,25}. The purpose of this study is to visualize and evaluate MF diffused into the cell walls of wood after conditioning at various RHs. Weight percent gain (WPG) and volumetric swelling behavior of the wood impregnated with an aqueous solution of MF were evaluated during conditioning at various RHs. The MF distribution in freeze-fixed samples after conditioning was visualized using cryo-TOF-SIMS. The conditioned wood was subsequently cured and a cross section was investigated using dry-TOF-SIMS.

Results and Discussion

WPG and relative swelling during conditioning. Figure 1a shows the temporal variability of WPG during conditioning at various RHs. At the start of the conditioning, which was 50 h before (Fig. 1a), the WPG decreased indicating water evaporation. Additionally, higher WPG was observed at higher RH, which is consistent with previous studies using PEG as the solute^{2,6}. This finding attributes to higher RH (higher vapor pressure) leading to slower water evaporation.

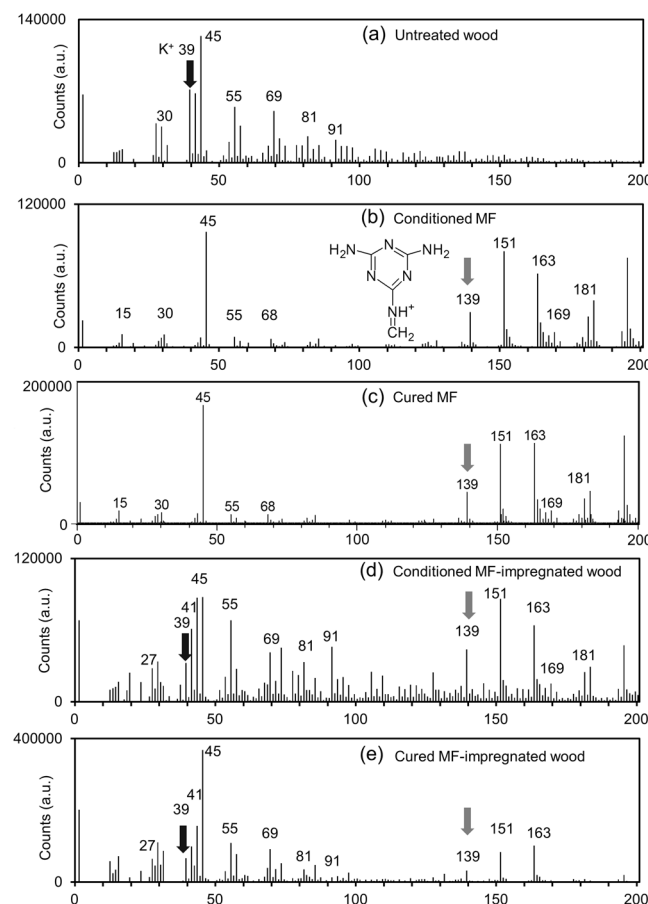


Figure 2. Positive ion TOF-SIMS spectra obtained from (a) untreated wood, (b) conditioned MF at RH of 43%, (c) cured MF, (d) conditioned MF-impregnated wood at RH of 43%, and (e) cured MF-impregnated wood. The characteristic peaks of K^+ at m/z 39 and the fragment MF ion at m/z 139 are shown. The structure of the fragment obtained from MF at m/z 139 is also inset in (b).

After 50 h of conditioning, the value of WPG at different RHs was similar and had reached equilibrium (Fig. 1a). However, the value of WPG after vacuum drying was significantly different ($P < 0.01$), i.e., $69.45\% \pm 0.26\%$, $66.64\% \pm 0.08\%$, and $61.02\% \pm 0.26\%$ for RHs of 11, 43 and 75%, respectively. These results indicate that MF itself degenerated during the conditioning and that the degeneration degree was RH dependent. Previous studies have revealed that polymerization can occur during the conditioning procedure for some resins because of dehydration, such as phenol formaldehyde resin^{26–28}. Additionally, higher RH can promote degradation^{26,27}. Similar polymerization might have occurred for MF in the present study, because MF polymerization also occurs as a result of dehydration¹³. The relative moisture content of the samples after conditioning, as calculated from the weight of the vacuum-dried samples, was significantly different ($P < 0.01$), i.e., $1.24\% \pm 0.03\%$, $6.23\% \pm 0.03\%$, and $15.76\% \pm 0.32\%$ for RHs of 11, 43 and 75%, respectively, which is consistent with previous studies using PEG as the solute².

Figure 1b shows the temporal variability of the volumetric relative swelling during the conditioning procedure at various RHs. Similar with temporal variability of the WPG (Fig. 1a), the relative swelling values decreased at the start of conditioning (Fig. 1b). As reported by previous research², the volumetric relative swelling values shown in Fig. 1b should be multiple results of swelling caused by MF diffusing into the cell walls and shrinkage caused by water exuding from the cell walls. A slower decrease in relative swelling was observed at higher RH at the start of conditioning (Fig. 1b), which is attributed to higher solute diffusivity and/or slower water exudation.

After 50 h, the relative swelling reached equilibrium and the samples at higher RH exhibited higher relative swelling (Fig. 1c). It is possible that the higher relative swelling was caused by the larger amount of MF diffusing into the cell walls at higher RH. On the other hand, as mentioned above, the samples at higher RH had a higher moisture content, which contributed to the cell wall swelling. Therefore, MF diffusion into the cell walls cannot be verified by the WPG and volumetric relative swelling results only.

Positive ion TOF-SIMS spectra. The typical positive ion spectra obtained from the untreated wood, conditioned MF at RH of 43%, cured MF, conditioned MF-impregnated wood at RH of 43%, and cured MF-impregnated wood in the mass region m/z of 0–200 are shown in Fig. 2a–e, respectively. Coullerez *et al.*²⁹ reported that m/z 139 ($[C_4H_7N_6]^+$), 151 ($[C_5H_7N_6]^+$), 163 ($[C_6H_7N_6]^+$), and 181 ($[C_6H_9N_6O]^+$) are the main characteristic peaks for both uncured and cured MF in a TOF-SIMS measurement. However, it was reported that

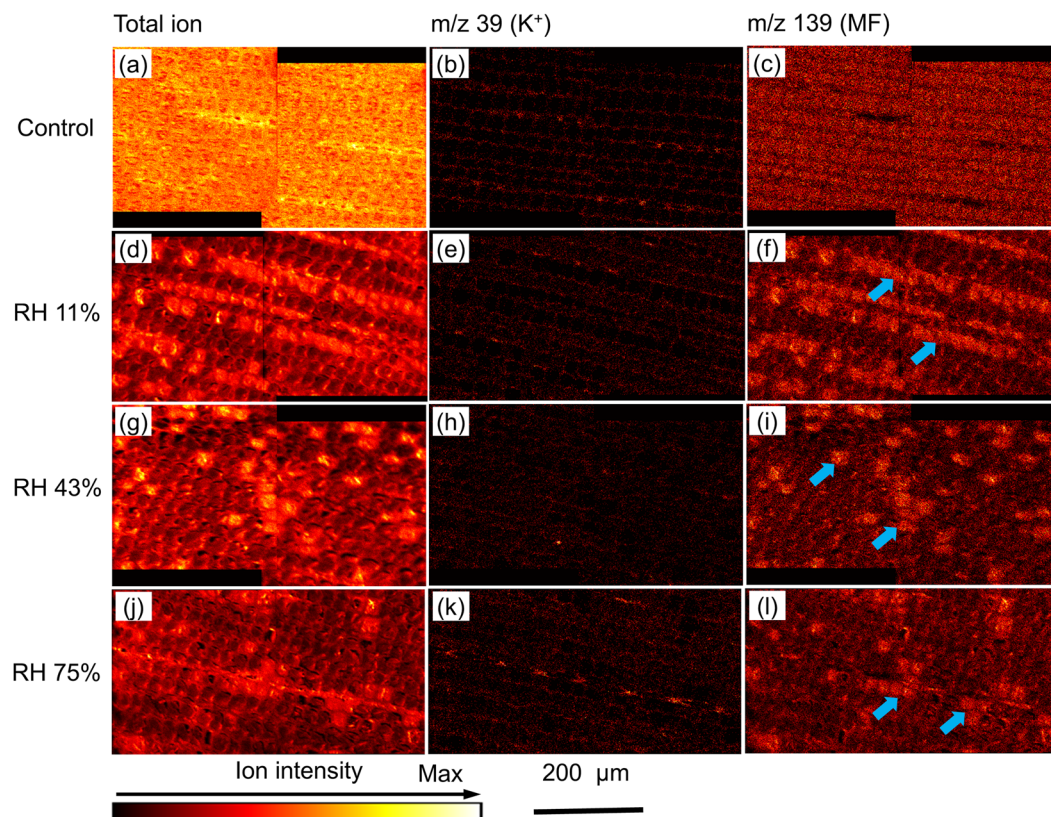


Figure 3. Cryo-TOF-SIMS images of the freeze-fixed MF-impregnated wood without conditioning (a–c; control), and with conditioning at RH of 11% (d–f), 43% (g–i), and 75% (j–l). The images of the total ion, m/z 39 (K^+), and m/z 139 (MF) are shown. Arrows indicate the cell cavities filled with MF.

m/z 151 ($[C_8H_7O_3]^+$ and $[C_9H_{11}O_2]^+$), 163 ($H^+ (H_2O)_n$), and 181 ($H^+ (H_2O)_n$ or $[C_9H_9O_4]^+$ and $[C_{10}H_{13}O_3]^+$) are also typical for lignins or water cluster ions in wood samples^{15–17,30}, which overlap with the MF characteristic peaks. Thus, the peak of m/z 139 ($[C_4H_7N_6]^+$) in the MF-impregnated wood samples investigated here is assigned as the characteristic peak of MF.

On the other hand, the signal m/z 39 is assigned to K^+ , which is mainly from wood cell walls. Moreover, inorganic K^+ (exact m/z 38.96) is distinguishable from organic C_3H_3 (exact m/z 39.02) in image mode as shown in our previous study¹⁵. Therefore, the peak of m/z 39 (K^+) was used to map the wood cell walls as reported in many previous studies^{23,24,33}.

MF distribution in conditioned MF-impregnated wood by cryo-TOF-SIMS. Representative cryo-TOF-SIMS images of the freeze-fixed MF-impregnated wood without conditioning (Figures a–c; control) or with conditioning at a RH of 11% (Figures d–f), 43% (Figures g–i), and 75% (Figures j–l) are shown in Fig. 3. The images of the total ions, m/z 39 (K^+), and m/z 139 (MF) are arranged on the left, middle, and right side, respectively (Fig. 3). The intracellular regions were filled by MF and/or water (as shown in Fig. 3a,d,g and j). Although the cell walls were clearly illustrated by mapping K^+ in the control sample (Fig. 3b), K^+ diffused into the cell cavity with the conditioning process (Fig. 3e,h and k).

In the MF-impregnated wood without conditioning, almost all the cell cavities were filled with the MF solution (Fig. 3c). The relative intensity of MF in the cell cavities was higher than that in the cell walls. This is because in comparison to the cell walls, the cell cavities can be more easily permeable to the MF solution in the impregnation process.

During the conditioning procedure at RH of 11%, a number of lines of cell cavities were filled with MF (Fig. 3f, arrows). With increase in RH, the numbers of cell cavities filled with MF decreased (Fig. 3i and l, arrows). Figure 4 shows the percentage of cell cavities filled with MF as calculated from the cryo-TOF-SIMS images (Fig. 3). It shows that a significantly lower percentage of cell cavities were filled with MF at higher RH (Fig. 4, $P < 0.01$), which indicates higher amounts of MF diffusing into the cell walls. These results are consistent with previous studies^{2,11}.

Previous studies reported that the amount of solute diffusion into the cell wall is determined by the difference of solute concentration between the walls and the cell cavities and solute diffusivity into the cell walls^{2,6,10}. At lower RH, the higher evaporation rate of water results in a larger concentration difference between the cell walls and the cell cavities. However, lower RH reduces the solute diffusivity into the cell walls^{2,11}. From the results of the present study, it can be concluded that the RH effect on solute diffusivity is greater than that on concentration difference between the cell walls and cell cavities during the conditioning process. Therefore, optimizing the RH

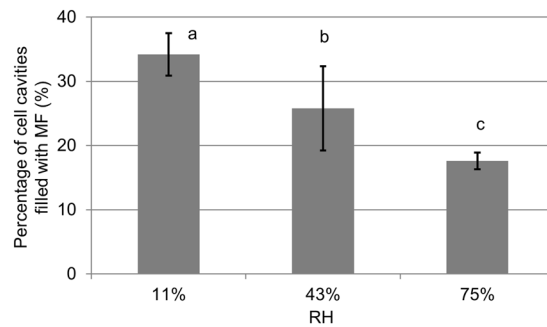


Figure 4. Percentage of cell cavities filled with MF as evaluated from the cryo-TOF-SIMS images in Fig. 3. The bars indicate the standard deviation from five replicates. Different letters indicate significant differences ($P < 0.01$).

to find a balance between the two factors (i.e. solute diffusivity and concentration difference between cell walls and cell cavities) is necessary for ensuring treatment efficiency.

MF distribution in cured MF-impregnated wood by dry-TOF-SIMS. The total ion and m/z 139 of MF are clearly mapped in Fig. 5. From the results, it is evident that MF was mainly located in the cell walls (Fig. 5b,d and f). The MF solution in the cell cavities was reduced because of water evaporation and MF polymerization, and deposited on the inner surface of the cell wall during drying and curing processes (Fig. 5b,d and f, arrows). It was difficult to evaluate the MF amount differences among various RHs only by checking the brightness of the images.

Thus, region-of-interest (ROI) function of TOF-SIMS was employed. Typical ROIs of the cell walls are enclosed with blue lines in Fig. 5a,c and e. The relative amount of MF-related ions was well quantified based on the total ions (Fig. 6), i.e., by dividing the MF (m/z 139) ion counts by the total ion counts. Figure 6 illustrates that the relative intensity of MF in the cell walls at RH of 75% was significantly higher than that at RH of 11 and 43% ($P < 0.01$). This means more MF diffused from cell cavity into cell wall at RH of 75%, which is consistent with less MF in cell cavity of the cryo-TOF-SIMS results (Figs 3 and 4). On the other hand, there is insignificant difference between the results at RH of 11 and 43% (Fig. 6). In Fig. 4, the standard deviation is large at RH of 43%, which indicates that the MF distribution is uneven between the different regions. This may have caused the insignificant difference between the results at RH of 11 and 43% in Fig. 6. Additionally, the limitations of TOF-SIMS due to ionization efficiency and the so-called matrix effect may be another factor^{16,17,31}.

From the representative photographs of MF-impregnated wood after conditioning at various RHs and subsequent vacuum drying (shown in Fig. 7), it is evident that there was a larger amount of MF exuding from the sample surface accompanied by bubbles at lower RH. The MF in the cell cavities can exude from the sample surface under vacuum condition. In another hand, MF in the cell walls fills the amorphous regions⁶ and is polymerized by dehydration^{13,26–28}, which is difficult to exude from the sample surface. Therefore, this result shows that there was a larger amount of MF in the cell cavities rather than the cell walls at lower RH, which confirms the TOF-SIMS results (Figs 3–6).

Conclusions

The MF distribution of impregnated and subsequently conditioned wood under various RHs was visualized using cryo- and dry-TOF-SIMS. Measurement of the dimensional variability showed a larger volumetric relative swelling of the cell walls at higher RH. Cryo-TOF-SIMS showed that more cell cavities remained unfilled by MF at higher RH, which indicates more MF diffusion into the cell walls. The relative intensity of MF in the cell walls was evaluated by dry-TOF-SIMS and the results showed that there was a larger amount of MF in the cell walls at higher RH.

TOF-SIMS has the ability to detect molecular or fragment ions of MF and subsequently map their distribution on the solution-impregnated sample surface with microscopic lateral resolution. A semi-quantitative evaluation of MF in the cell walls can be performed. TOF-SIMS will be a powerful tool for future studies of solute diffusion mechanisms in solution-impregnated wood.

Methods

Sample treatment. Wood samples were prepared from a block of *Chamaecyparis obtusa* with nominal dimensions of 5 mm × 25 mm × 25 mm in the longitudinal, radial, and tangential directions, respectively. The samples were dried at 105 °C to a constant mass, followed by measurement of their weights (W_0) and dimensions (V_0). The density of the dry samples was uniform (0.41 ± 0.002 g cm⁻³).

The oven-dried samples were soaked in a 30% aqueous solution of MF [Beckamine M-3 (60), DIC Corporation, Osaka, Japan; average molecular weight: approximately 350] under vacuum at a pressure of 0.01 MPa for 2 h and subsequently subjected to a pressure at 0.8 MPa for 18 h in an impregnation plant (YA-10, Yasujima, Kanazawa, Japan). The impregnated samples were blotted and their weights and dimensions were measured.

The samples were divided equally into four groups. One group was immediately frozen in liquid Freon R22 (DuPont) at -160 °C without conditioning and stored at -80 °C. The other groups were conditioned for 125 h in a desiccator (MD-1, Sanplatec, Osaka, Japan) at RHs of 11, 43, or 75% (at 35 °C) using supersaturated solutions of

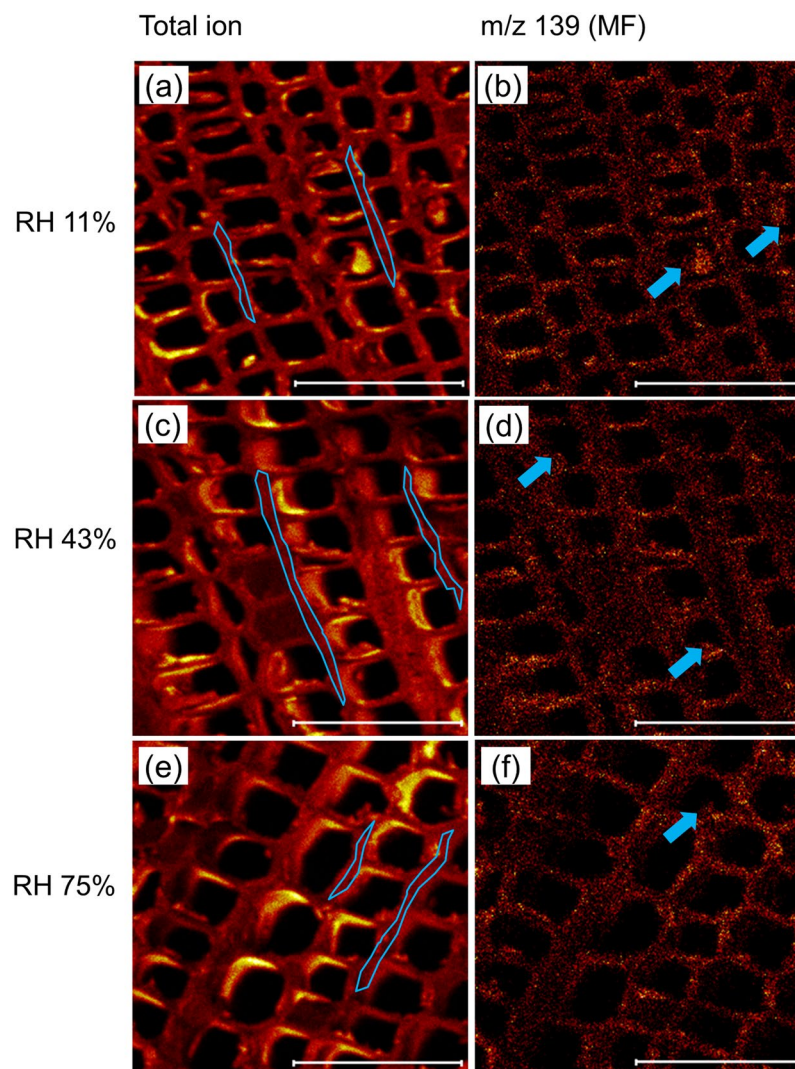


Figure 5. Representative total ion images and MF distribution maps of the cured samples conditioned under RH of 11% (a and b), 43% (c and d), and 75% (e and f). The typical ROIs of the cell walls are enclosed with blue lines. Arrows indicate MF deposited on the inner surface of the cell walls. Scale bar: 100 μm.

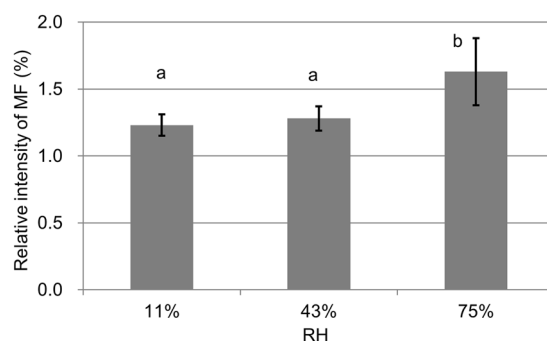


Figure 6. Relative intensity of MF in the cell wall of the cured samples as shown in Fig. 5. The bars represent standard deviation from five replicates. Different letters indicate significant differences ($P < 0.01$).

lithium chloride (LiCl), potassium carbonate (K_2CO_3), and sodium chloride (NaCl), respectively³². The weights (W_i) and dimensions (V_i) of the samples were measured frequently during the conditioning procedure. The WPG and the volumetric relative swelling of the samples during conditioning procedures were then calculated using the equations 1 and 2 respectively:

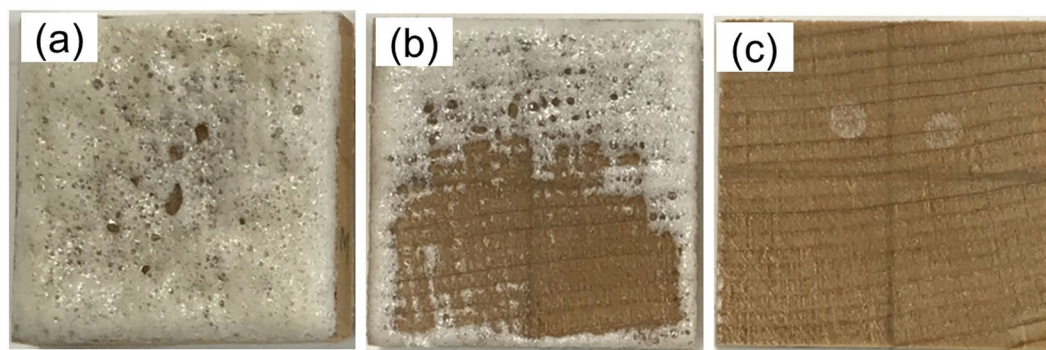


Figure 7. Representative photographs of the MF-impregnated wood after conditioned at RH of 11% (a), 43% (b), and 75% (c), and subsequently vacuum dried.

$$\text{WPG} = (W_i - W_0)/W_0 \times 100\% \quad (1)$$

$$\text{Relative swelling} = (V_i - V_0)/V_0 \times 100\% \quad (2)$$

Half of the conditioned samples were immediately frozen in liquid Freon R22 (DuPont) at -160°C and stored at -80°C . The other half were dried in a vacuum chamber (at 0.01 MPa and 35°C) for 48 h and cured (at atmospheric pressure and 170°C) for 1 h. The frozen and cured samples were prepared for cryo- and dry-TOF-SIMS (ULVAC-PHI, Inc., Kanagawa, Japan), respectively.

Cryo-TOF-SIMS measurement. Four kinds of frozen sample blocks (i.e., the impregnated samples and the conditioned samples at RHs of 11, 43, and 75%) were cut and set to the sample holder with ice. Then a clean and even cross surface of the samples was cut in a glove box, where the temperature was controlled at -30°C by cooled nitrogen gas to prevent water sublimation. Subsequently, the samples were transferred to the cryo-TOF-SIMS for measurement. Details of the cryo-TOF-SIMS system have been reported by Kuroda *et al.*³³ and Masumi *et al.*³⁴.

During the cryo-TOF-SIMS measurement, the samples were maintained at lower than -120°C . Positive ion spectra were collected under the following conditions: primary ion, 22 keV Au_1^+ at a current of 5 nA; pulse width, 13 ns for unbunched image analysis, and 1.8 ns for bunched spectrum analysis. A low-energy pulsed electron gun (30.0 eV) was used for surface charge compensation¹⁵. The measured surface areas were $300 \times 300 \mu\text{m}^2$ and the total ion counts were approximately 8×10^6 with an acquisition time of 10 min for each image.

Dry-TOF-SIMS measurement. The measurement conditions of dry-TOF-SIMS were similar to that of cryo-TOF-SIMS. The measured surface areas were $200 \times 200 \mu\text{m}^2$ and the total ion counts were approximately 3×10^6 with an acquisition time of 10 min for each image. The ROIs of the cell walls were selected to evaluate the relative intensity of MF.

Statistical analysis. Significance of the differences between the samples conditioned under various RHs was evaluated by a Statistical Product and Service Solutions (SPSS 24.0, IBM), which included analysis of one-way ANOVA followed by Tukey tests at the 99% confidence level.

Data availability. All data generated or analysed during this study are included in this published article.

References

- Gierlinger, N. *et al.* Comparison of UV and confocal Raman microscopy to measure the melamine-formaldehyde resin content within cell walls of impregnated spruce wood. *Holzforschung* **59**, 210–213 (2005).
- Tanaka, S., Seki, M., Miki, T., Shigematsu, I. & Kanayama, K. Solute diffusion into cell walls in solution-impregnated wood under conditioning process I: effect of relative humidity on solute diffusivity. *J. Wood Sci.* **61**, 543–551 (2015).
- Furuno, T., Imamura, Y. & Kajita, H. The modification of wood by treatment with low molecular weight phenol-formaldehyde resin: a properties enhancement with neutralized phenolic-resin and resin penetration into wood cell walls. *Wood Sci. Technol.* **37**, 349–361 (2004).
- Norimoto, M. & Grill, J. Structure and properties of chemically treated wood in Recent research on wood and wood-based materials, Current Japanese materials research, vol. 11 (eds Shiraishi, N., Kajita, H. & Norimoto, M.) 135–154 (Elsevier Applied Science, 1993).
- Rowell, R. M. & Banks, W. B. Water repellency and dimensional stability of wood. *USDA General Technical Report FPL* **50**, 1–24 (1985).
- Tanaka, S., Seki, M., Miki, T., Shigematsu, I. & Kanayama, K. Solute diffusion into cell walls in solution-impregnated wood under conditioning process II: effect of solution concentration on solute diffusion. *J. Wood Sci.* **62**, 146–155 (2016).
- Furuno, T. & Goto, T. Structure of the interface between wood and synthetic polymer (XI). The role of polymer in the cell wall on the dimensional stability of wood-polymer composite (WPC). *Mokuzai Gakkaishi* **24**, 287–293 (1978).
- Furuno, T. & Goto, T. Structure of the interface between wood and synthetic polymer (XII). Distribution of styrene polymer in the cell wall of wood-polymer composite (WPC) and dimensional stability. *Mokuzai Gakkaishi* **25**, 488–495 (1979).

9. Tanaka, S., Seki, M., Miki, T., Umemura, K. & Kanayama, K. Solute diffusion into cell walls in solution-impregnated wood under conditioning process III: effect of relative humidity schedule on solute diffusion into shrinking cell walls. *J. Wood Sci.* **63**, 263–270 (2017).
10. Stamm, A. J. Dimensional stabilization of wood with carbonwaxes. *For. Prod. J.* **6**, 201–204 (1956).
11. Stamm, A. J. Factors affecting the bulking and dimensional stabilization of wood with polyethylene glycols. *For. Prod. J.* **14**, 403–408 (1964).
12. Schneider, V. A. Contribution on the dimensional stabilization of wood with polyethylene glycol—part 1: basic investigation on the dimensional stabilization of wood with polyethylene glycol (in German). *Holz Roh Werkst* **27**, 209–224 (1969).
13. Merline, D. J., Vukusic, S. & Abdala, A. A. Melamine formaldehyde: curing studies and reaction mechanism. *Polym. J.* **45**, 413–419 (2013).
14. Vickerman, J. C. & Briggs, D. TOF-SIMS: Surface Analysis by Mass Spectrometry (IM Publications and Surface Spectra Limited, 2001).
15. Zheng, P. *et al.* Determination of inorganic element distribution in the freeze-fixed stem of *Al₂(SO₄)₃-treated Hydrangea macrophylla* by TOF-SIMS and ICP-AES. *Holzforschung* **71**, 471–480 (2017).
16. Zheng, P. *et al.* Lignification of ray parenchyma cells in xylem of *Pinus densiflora*. Part I: Microscopic investigation by POM, UV microscopy, and TOF-SIMS. *Holzforschung* **68**, 897–905 (2014).
17. Zheng, P. *et al.* Lignification of ray parenchyma cells (RPCs) in the xylem of *Phellodendron amurense* Rupr. quantitative and structural investigation by TOFSIMS and thioacidolysis of laser microdissection cuts of RPCs. *Holzforschung* **70**, 641–652 (2016).
18. Vanbellingen, Q. P. *et al.* Analysis of chemotherapeutic drug delivery at the single cell level using 3D-MSI-TOF-SIMS. *J. Am. Soc. Mass Spectrom.* **27**, 2033–2040 (2016).
19. Bich, C., Touboul, D. & Brunelle, A. Study of experimental variability in TOF-SIMS mass spectrometry imaging of biological samples. *Int. J. Mass Spectrom.* **337**, 43–49 (2013).
20. Kajiwara, Y. *et al.* Multivariate analysis and g-ogram application to ToF-SIMS data of PEG mixed model sample. *Surf. Interface Anal.* **46**, 1183–1186 (2014).
21. Shon, H. K. *et al.* ToF-SIMS imaging and spectroscopic analyses of PEG-conjugated AuNPs. *Surf. Interface Anal.* **43**, 628–631 (2011).
22. Vanbellingen, Q. P. *et al.* Mapping *Dicorynia guianensis* Amsh. wood constituents by submicron resolution cluster-TOF-SIMS imaging. *J. Mass Spectrom.* **51**, 412–423 (2016).
23. Aoki, D. *et al.* Distribution of coniferin in freeze-fixed stem of *Ginkgo biloba* L. by cryo-TOF-SIMS/SEM. *Sci. Rep.* **6**, 31525 (2016).
24. Aoki, D. *et al.* Translocation of ¹³³Cs administered to *Cryptomeria japonica* wood. *Sci. Total Environ.* **584–585**, 88–95 (2017).
25. Bajia, S., Sharma, R. & Bajia, B. Solid-state microwave synthesis of melamine formaldehyde resin. *J. Chem.* **6**, 120–124 (2009).
26. Lorenz, L. F. & Christiansen, A. W. Interactions of phenolic resin alkalinity, moisture content, and cure behaviour. *Znd. Eng. Chem. Res.* **34**, 4520–4523 (1995).
27. Seki, M. *et al.* Extrusion of solid wood impregnated with phenol formaldehyde (PF) resin: effect of resin content and moisture content on extrudability and mechanical properties of extrudate. *BioResources* **11**, 7697–7709 (2016).
28. Valdez, D., & Nagy, E. Analyses/Testing in Phenolic resins: a century of progress (ed. Polato, L.) 93–138 (Springer, 2010).
29. Coullerez, G., Léonard, D., Lundmark, S. & Mathieu, H. J. XPS and ToF-SIMS study of freeze-dried and thermally cured melamine–formaldehyde resins of different molar ratios. *Surf. Interface Anal.* **29**, 431–443 (2000).
30. Saito, K., Kato, T., Tsuji, Y. & Fikushima, K. Identifying the characteristic secondary ions of lignin polymer using TOF-SIMS. *Biomacromolecules* **6**, 678–683 (2005).
31. Rabbani, S., Barber, A. M., Fletcher, J. S., Lockyer, N. P. & Vickerman, J. C. TOF-SIMS with argon gas cluster ion beams: a comparison with C₆₀⁺. *Anal. Chem.* **83**, 3793–3800 (2011).
32. Greenspan, L. Humidity fixed points of binary saturated aqueous solutions. *Journal of Research of the National Bureau of Standards—A. Physics and Chemistry* **81A**, 89–96 (1977).
33. Kuroda, K. *et al.* The cryo-TOF-SIMS/SEM system for the analysis of the chemical distribution in freeze-fixed *Cryptomeria japonica* wood. *Surf. Interface Anal.* **45**, 215–219 (2013).
34. Masumi, T. *et al.* Adsorption behavior of poly (dimethyl-diallylammonium chloride) on pulp fiber studied by cryo time-of-flight secondary ion mass spectrometry and cryo-scanning electron microscopy. *Appl. Surf. Sci.* **289**, 155–159 (2014).

Acknowledgements

This work was supported by the Japan Society for the Promotion of Science KAKENHI (Nos 25252032 and 17H03842). We thank Ms. Yuko Yashima (Structural Materials Research Institute, National Institute of Advanced Industrial Science and Technology, Nagoya, Japan) for support with sample treatment and Editage (<https://online.editage.jp/>) for its linguistic assistance during the preparation of this manuscript.

Author Contributions

All authors conceptualized and designed the research; D.A. and P.Z. conducted the TOF-SIMS measurements and analysed data; P.Z., D.A., M.S., and S.T. wrote the manuscript; all authors reviewed the manuscript.

Additional Information

Competing Interests: The authors declare no competing interests.

Publisher's note: Springer Nature remains neutral with regard to jurisdictional claims in published maps and institutional affiliations.



Open Access This article is licensed under a Creative Commons Attribution 4.0 International License, which permits use, sharing, adaptation, distribution and reproduction in any medium or format, as long as you give appropriate credit to the original author(s) and the source, provide a link to the Creative Commons license, and indicate if changes were made. The images or other third party material in this article are included in the article's Creative Commons license, unless indicated otherwise in a credit line to the material. If material is not included in the article's Creative Commons license and your intended use is not permitted by statutory regulation or exceeds the permitted use, you will need to obtain permission directly from the copyright holder. To view a copy of this license, visit <http://creativecommons.org/licenses/by/4.0/>.

© The Author(s) 2018